24th COBEM - 2017

24th ABCM International Congress of Mechanical Engineering
December 3-8, 2017, Curitiba, PR, Brazil

COBEM-2017-1448
AN INVESTIGATION ABOUT THE USE OF A CONSTANT ABSORPTION CROSS-SECTION FOR RADIATIVE HEAT TRANSFER COMPUTATIONS IN NONUNIFORM CO_2 GASES.

Gabriel de Lima Bernardino
André Jesus Soares Maurente
Laboratório de Sistemas Térmicos I, Departamento de Engenharia Mecânica, Universidade Federal do Rio Grande do Norte, Campus Universitário, Lagoa Nova, Natal, RN, 59090-970, Brazil
gabriellima050695@gmail.com, amaurente@gmail.com

Abstract. *Processes of heat transfer by radiation are very important in scientific and industrial applications. When these processes involve participating gases at high temperatures that emit and absorb radiation, radiant exchanges can become the main mechanism of heat transfer. The computation of the spectral absorption cross-section of CO_2 (which is essential to compute emission and absorption of radiation), requires a discretization of the spectrum in several spectral points. This work presents an analysis of the relation of CO_2 concentration with the absorption cross-section. Based on the HITEMP2010 database, the spectral absorption cross-section was calculated considering a uniform media with temperatures of 500 K, 1500 K and 2500 K and four different molar fractions of CO_2. An analysis was also accomplished for a non-isothermal medium. The results show that as the absorption cross-section is much less sensible to chemical species concentration than the absorption coefficient, a constant absorption cross section can be used in nonuniform gases composed of CO_2 and inert species with acceptable accuracy.*

Keywords: *Absorption cross-section, radiation heat transfer, spectral properties, HITEMP.*

1. INTRODUCTION

Radiation heat transfer in participating media (semitransparent media that emit and absorb thermal radiation) is an important mechanism for the analysis of many devices found in industries and in scientific studies. This analysis, in many engineering applications, must be performed in such a way that the spectral variation of radiative properties (variation in relation to wavenumber, wavelength or frequency) should be considered. All radiative properties may vary strongly with wavelength, adding another dimension to the governing equation (Modest, 2013).

Simulation of radiative heat transfer requires that the spectral radiative properties of the participating media be pre-calculated. In this work the effect of radiation scattering will not be considered. Thus, the properties involved in the studies will be the absorption coefficient and the absorption cross-section that are directly related to the emission and absorption of radiation by participating media. These properties are spectrally dependent and are obtained in this work from the HITEMP2010 database (Rothman et al., 2010). This database contains parameter for spectral lines of a series of molecules.

When the analysis is performed in non-homogeneous media, the necessary database about either the absorption coefficient or absorption cross-section used to be extensive, requiring considerably computational resources.

In this work it is presented an analysis about how the absorption cross-section varies with CO_2 concentration. This analysis was based on calculations of the radiative heat flux and the divergence of the radiative heat flux in homogeneous and isothermal media. Some approximations were presented for some concentrations in a non-isothermal and homogeneous media, considering a temperature profile presented by Solovjov and Webb (2010).

The finite volume method (Patankar, 1980) was used to compute the radiative heat flux and divergence of the radiative heat flux. The line-by-line method was used for spectral integration, which requires considerably computational time. Some models were implemented aiming at a faster calculation with good approximations.

Alternatively time consuming line-by-line method, there are approximated models for considering the spectral dependence of radiative properties. Some examples are the weighted-sum-of-gray gases (WSGG) (Hottel and Sarofim, 1967), spectral-line-based-weighted-sum-of-gray gases (SLW) (Denison and webb, 1993a; Denison, Lemonnie and Webb, 2011), absorption distribution function (ADF) (Rivière, Soufiani, Perrin, Riad and Gleizes, 1996; Pierrot, Soufiani and Taine,1999), cumulative wavenumber (CW) (Solovjov and Webb, 2002; Galarça, Mossi and França, 2011), full-

spectrum k-distribution (FSK) (Zhang and Modest, 2002a; Zhang and Modest, 2005) and the multi-scale FSCK (MSFSCK) (Zhang and Modest, 2002b). In all of this methods the model parameters are usually computed from the line-by-line spectral properties. Thus, the analysis presented here can be useful for line-by-line computations and when spectral models are being employed.

The analysis presented in this work shows that satisfactory results can be obtained by approximating the absorption cross-section, C_η, of media with varied CO_2 mole fraction as that obtained for a media constituted by 25 % CO_2.

2. CALCULATION AND ANALYSIS PROCEDURE

The absorption cross-section can be calculated according to Eq. (1) for most combustion problems (Denison and Webb, 1993b). The calculation was accomplished by discretizing the spectrum into 50.000 spectral points. The number of spectral points was found with a previous study of the convergence of the spectral absorption cross-section.

$$C_\eta = \sum_i \frac{S_i}{\pi} \frac{\gamma_i}{(\eta - \eta_i)^2 + \gamma_i^2} \tag{1}$$

Where S is the line strength, γ is the half width, η is the wavenumber and i is the index of the line. In the calculations performed in this work 11.193.608 lines were considered. S_i, γ_i and η_i are given for each line by the HITEMP2010 (Rothman et al., 2010) database.

The spectral absorption coefficient is related to C_η by Eq. (2) (Howell et al., 2016; Modest, 2013).

$$\kappa_\eta = C_\eta D \tag{2}$$

Where D is the molar density.

The intensity of a radiation ray propagating in a direction s is given by the Radiative Transfer Equation (RTE), which for an absorbing and emitting media, becomes:

$$\frac{dI_\eta}{ds} = \kappa_\eta I_{b,\eta} - \kappa_\eta I_\eta \tag{3}$$

where I_η is the spectral intensity of radiation, $I_{b,\eta}$ is the black body spectral intensity, given by the Planck function and ds is a differential element of length along the path of propagation of the radiation ray.

The total intensity is obtaining by integration over the entire spectrum, as shown in the Eq. (4).

$$I = \int_0^\infty I_\eta d\eta \tag{4}$$

The heat flux in a one-dimensional media layer, whose properties vary only in the x direction, as considered in this work, is obtained by Eq. (5).

$$q_{r,x} = \int_0^{4\pi} I(\Omega) cos(\theta) d\Omega \tag{5}$$

Where Ω is the solid angle.

Equations (3-5) where numerically solved using the finite volume method accordingly to the procedure presented by Patankar (1980).

The analysis of the variation of the absorption cross-section with CO_2 concentration in the radiative heat flux and divergence of the radiative heat flux computations was performed considering isothermal and uniform media. Four different CO_2 mole fractions and three different temperatures were considered: 5 %, 50 %, 75 % and 100 %, and 500 K, 1500 K and 2500 K. The same analysis was performed for a non-isothermal and homogeneous media. In this case, the spectral absorption coefficients were calculated for the temperatures of 500 K, 1000 K, 1500 K and 2000 K, and the absorption coefficients for intermediate temperatures were obtained by interpolation.

For each considered temperature, the absorption coefficient was calculated for each temperature based on the concentrations of 5 %, 50 %, 75 % and 100 %. Results were obtained with the real absorption coefficient, which was calculated from the real CO_2 concentration for both absorption-cross section and number density, while the approximated results were obtained with an absorption coefficient computed with the number density computed from the real CO_2 concentration and an absorption-cross section computed considering a fixed CO_2 concentration equal to 25 %.

The heat flux and the divergence of the heat flux were computed using the real and the approximated absorption coefficient. The real results were obtained based on the real absorption coefficients and the approximate ones based on the approximate absorption coefficients. The analysis consisted on comparing the real and approximate results for each temperature and concentration (isothermal and uniform media), and the errors were calculated as given by Eq. 6 and Eq. 7.

$$Error = \frac{q_{real} - q_{approximated}}{|highest(q_{real})|} \tag{6}$$

$$Error = \frac{d_{real} - d_{approximated}}{|highest(d_{real})|} \tag{7}$$

Where q is the heat flux and d is the divergence of the heat flux. The denominator is maximum value due to the fact that the division by zero or very small values is not desirable. Figure 1 outlines the whole process.

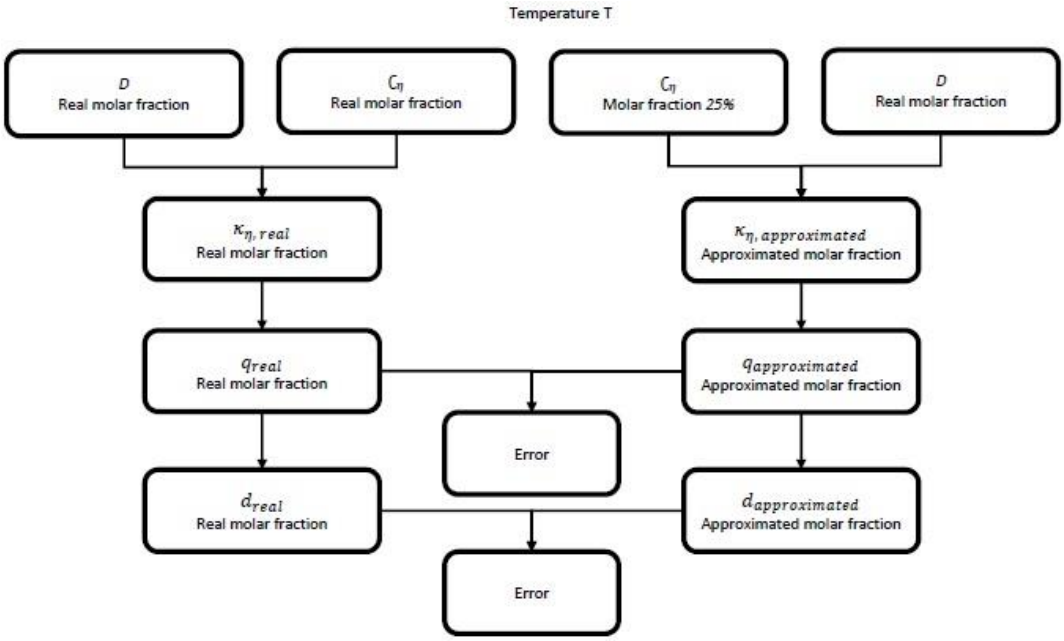

Figure 1. Analysis scheme.

3. RESULTS AND DISCUSSION

As an example, the absorption coefficient for the temperature of 1500 K and concentration of 25 % computed using that from HITEMP2010 (Rothman, et al, 2010) database is shown in Fig. 2.

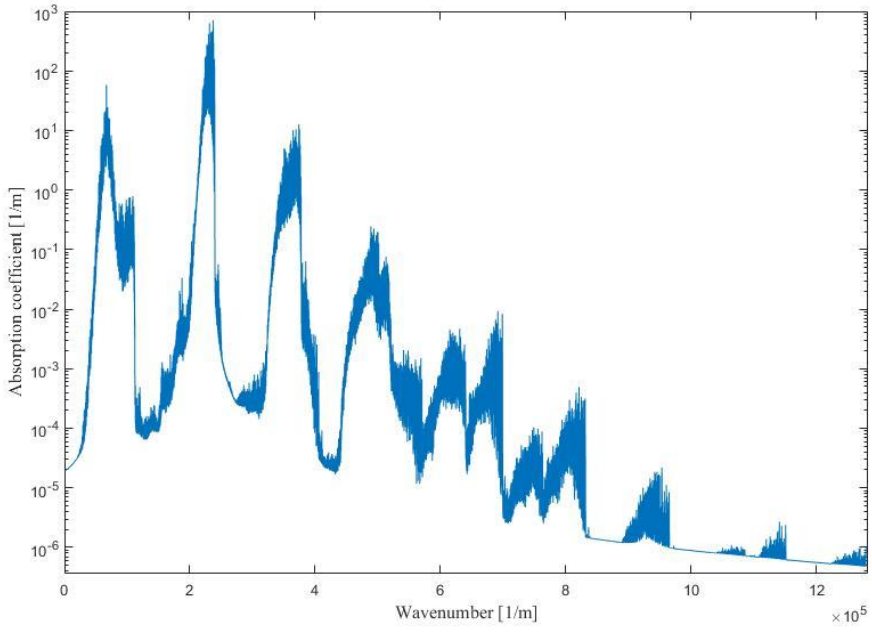

Figure 2. Absorption coefficient versus wavenumber.

The results for the heat flux and the error associated with the approximation for a homogeneous and isothermal layer with length L = 1 m and wall temperatures of 300 K for medium temperature of 500 K and concentration of 5 %, 50 %, 75 % and 100 % are presented in Fig. 3.

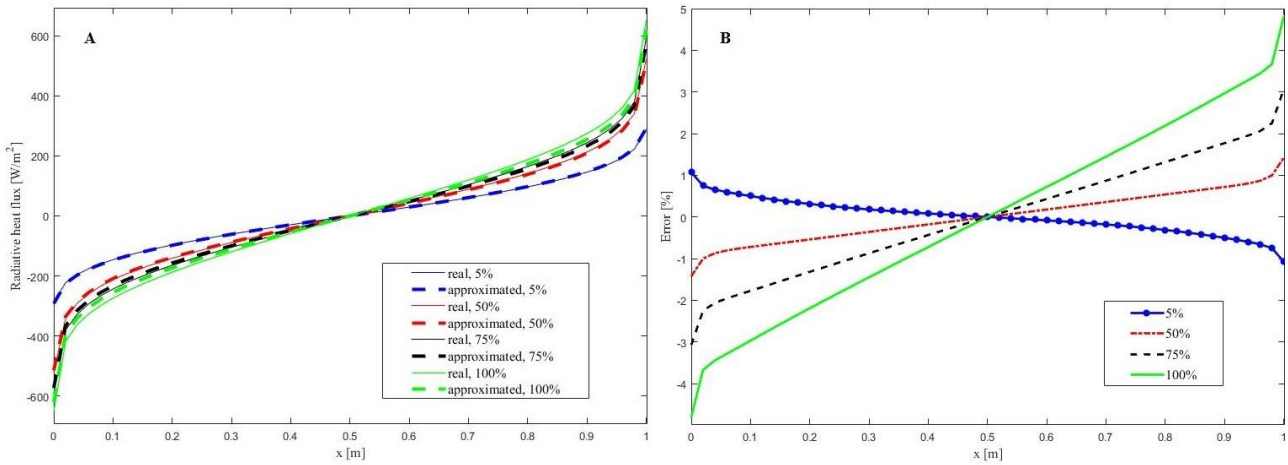

Figure 3. Heat flux (A) and error (B) for temperature of 500 K and concentrations of 5 %, 50 %, 75 % and 100 %.

The average, standard deviation, maximum and minimum values related to the error shown in Fig. 3 are in Tab. 1.

Table 1. Error data associated with the approximation of the heat flux for a homogeneous and isothermal medium for 500 K.

Molar fraction	Average error (%)	Standard deviation of the error	Maximum error (%)	Minimum error (%)
5 %	0.2960	0.2344	1.0733	3.9387×10^{-14}
50 %	0.4674	0.2988	1.4255	2.1792×10^{-14}
75 %	1.1228	0.6915	3.0694	3.8483×10^{-14}
100%	1.8639	1.1346	4.8089	0

The results for the heat flux and the error associated with the approximation for a homogeneous and isothermal layer with length L = 1 m and wall temperatures of 300 K for medium temperature of 1500 K and concentration of 5 %, 50 %, 75 % and 100 % are presented in Fig. 4.

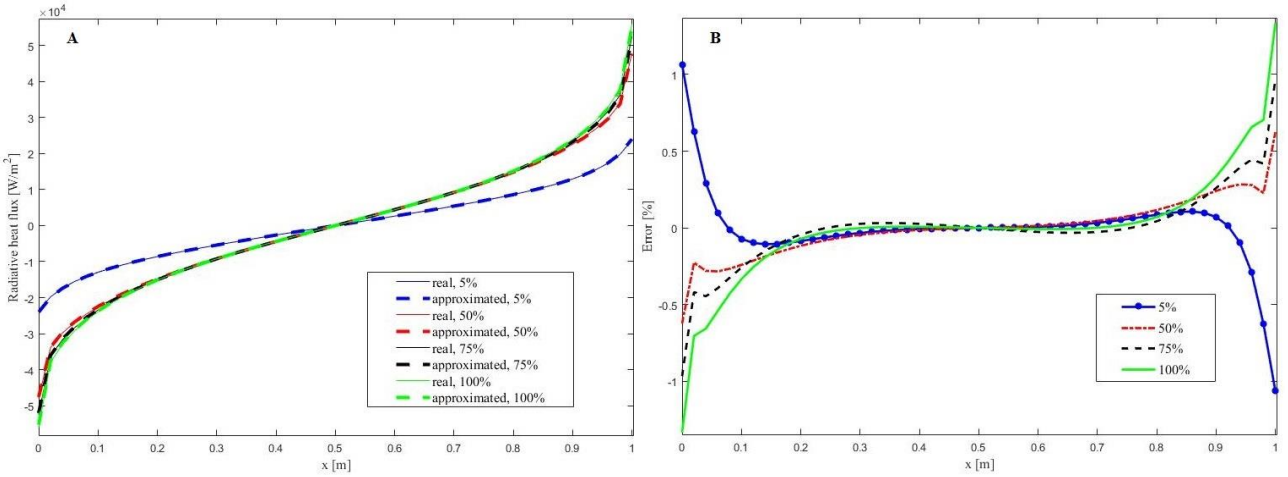

Figure 4. Heat flux (A) and error (B) for temperature of 1500 K and concentrations of 5 %, 50 %, 75 % and 100 %.

The average, standard deviation, maximum and minimum values related to the error shown in Fig. 4 are in Tab. 2.

Table 2. Error data associated with the approximation of the heat flux for a homogeneous and isothermal medium for 1500 K.

Molar fraction	Average error (%)	Standard deviation of the error	Maximum error (%)	Minimum error (%)
5 %	0.0987	0.1873	1.0634	3.0617×10^{-14}
50 %	0.1166	0.1201	0.6236	1.5184×10^{-14}
75 %	0.1274	0.1845	0.9674	1.3845×10^{-14}
100%	0.1698	0.2702	1.3338	0

The results for the heat flux and the error associated with the approximation for a homogeneous and isothermal layer with length L = 1 m and wall temperatures of 300 K for medium temperature of 2500 K and concentration of 5 %, 50 %, 75 % and 100 % are presented in Fig. 5.

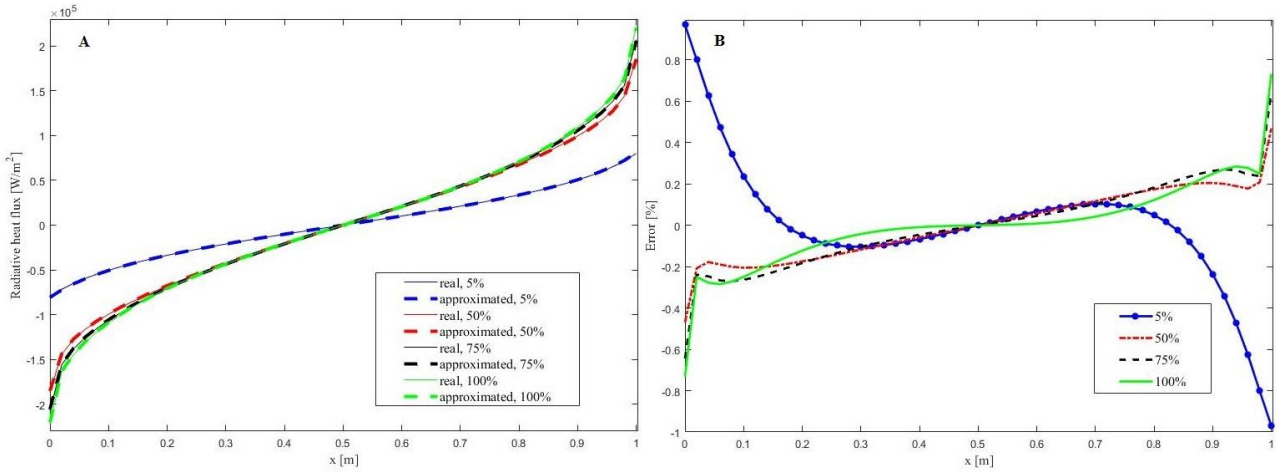

Figure 5. Heat flux (A) and error (B) for temperature of 2500 K and concentrations of 5 %, 50 %, 75 % and 100 %.

The average, standard deviation, maximum and minimum values related to the error shown in Fig. 5 are in Tab. 3.

Table 3. Error data associated with the approximation of the heat flux for a homogeneous and isothermal medium for 2500 K.

Molar fraction	Average error (%)	Standard deviation of the error	Maximum error (%)	Minimum error (%)
5 %	0.1726	0.2257	0.9709	0
50 %	0.1359	0.0807	0.4690	0
75 %	0.1516	0.1135	0.6444	0
100%	0.1206	0.1332	0.7323	1.3109×10^{-14}

The results of the divergence of the heat flux and the error associated with the approximation for a homogeneous and isothermal layer with length L = 1 m and wall temperatures of 300 K for medium temperature of 500 K and concentration of 5 %, 50 %, 75 % and 100 % are presented in Fig. 6.

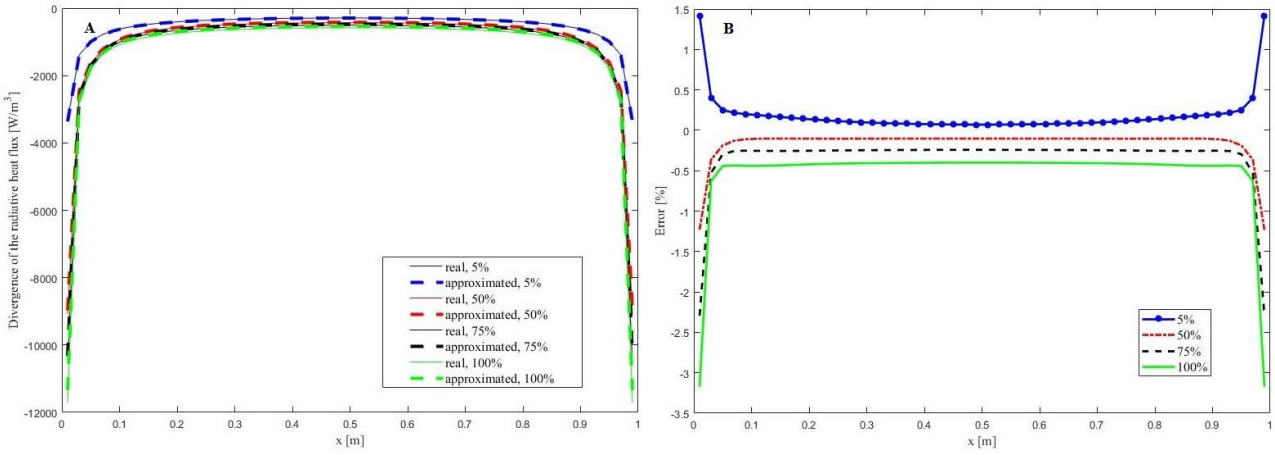

Figure 6. Divergence of the heat flux (A) and error (B) for temperature of 500 K and concentrations of 5 %, 50 %, 75 % and 100 %.

The average, standard deviation, maximum and minimum values related to the error shown in Fig. 6 are in Tab. 4.

Table 4. Error data associated with the approximation for divergence of the heat flux for a homogeneous and isothermal medium for 500 K.

Molar fraction	Average error (%)	Standard deviation of the error	Maximum error (%)	Minimum error (%)
5 %	0.1865	0.2618	1.4171	0.0699
50 %	0.1636	0.2245	1.2325	0.1026
75 %	0.3433	0.4020	2.2941	0.242
100%	0.5351	0.5405	3.1744	0.4009

The results for the divergence of the heat flux and the error associated with the approximation for a homogeneous and isothermal layer with length L = 1 m and wall temperatures of 300 K for media temperature of 1500 K and concentration of 5 %, 50 %, 75 % and 100 % are presented in Fig. 7.

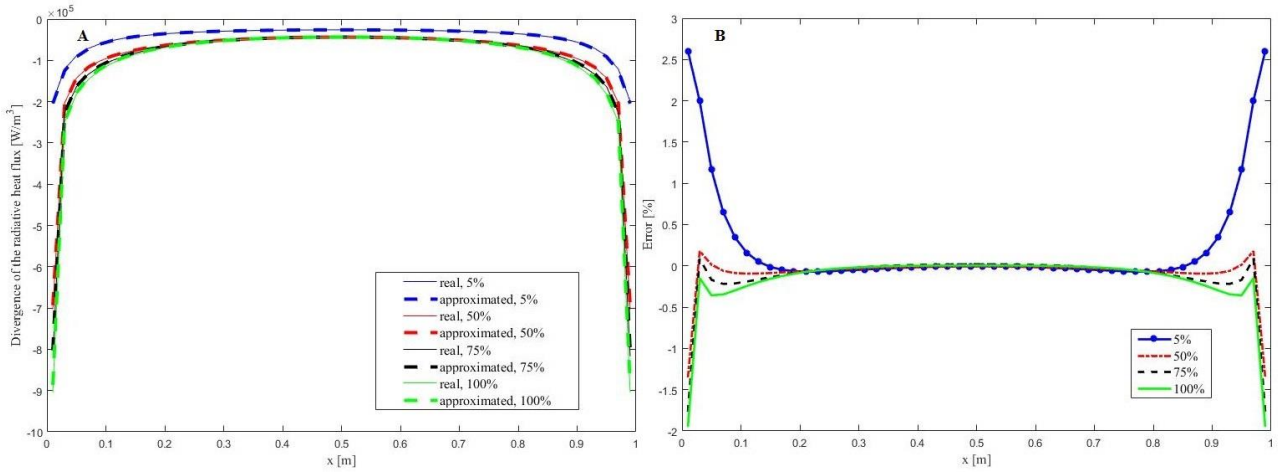

Figure 7. Divergence of the heat flux (A) and error (B) for temperature of 1500 K and concentrations of 5 %, 50 %, 75 % and 100 %.

The average, standard deviation, maximum and minimum values related to the error shown in Fig. 7 are in Tab. 5.

Table 5. Error data associated with the approximation for divergence of the heat flux for a homogeneous and isothermal medium for 1500 K.

Molar fraction	Average error (%)	Standard deviation of the error	Maximum error (%)	Minimum error (%)
5 %	0.3040	0.6453	2.6031	0.0050
50 %	0.1004	0.2585	1.3521	0.0073
75 %	0.1396	0.3391	1.7658	0.0011
100%	0.1671	0.3804	1.9502	0.0011

The results for the divergence of the heat flux and the error associated with the approximation for a homogeneous and isothermal layer with length L = 1 m and wall temperatures of 300 K for medium temperature of 2500 K and concentration of 5 %, 50 %, 75 % and 100 % are presented in Fig. 8.

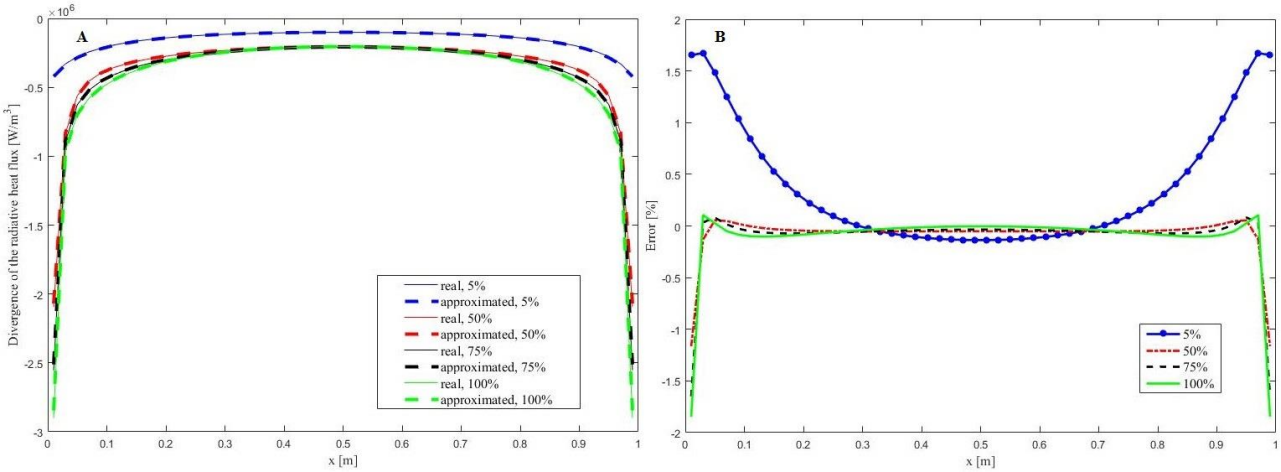

Figure 8. Divergence of the heat flux (A) and error (B) for temperature of 2500 K and concentrations of 5 %, 50 %, 75 % and 100 %.

The average, standard deviation, maximum and minimum values related to the error shown in Fig. 8 are in Tab. 6.

Table 6. Error data associated with the approximation for divergence of the heat flux for a homogeneous and isothermal medium for 2500 K.

Molar fraction	Average error (%)	Standard deviation of the error	Maximum error (%)	Minimum error (%)
5 %	0.4549	0.5324	1.6735	0.0061
50 %	0.0931	0.2196	1.1643	0.0034
75 %	0.1150	0.3133	1.6482	0.0152
100%	0.1227	0.3535	1.8463	0.0038

The results for the heat flux and the error associated with the approximation for a homogeneous and non-isothermal layer with length L = 0.2 m, temperature distribution of $T(x) = 1000+250\cos(\pi x/2)$ in Kelvin and wall temperatures of T_0 = 1750 K and T_L = 750 K presented by solovjov and Webb (2009), are presented in Fig. 9 for molar fractions of 5 %, 50 %, 75 % and 100%.

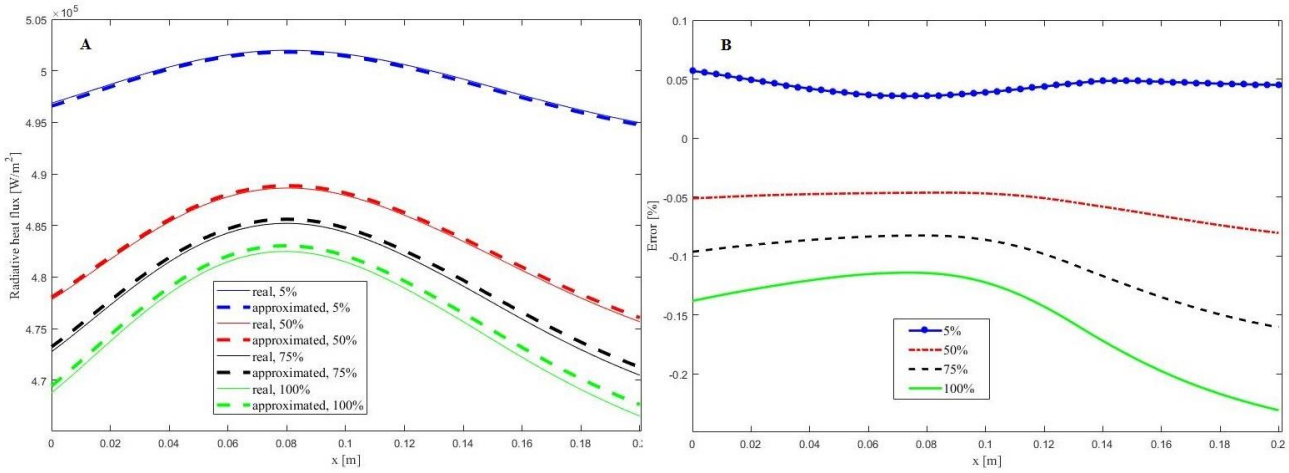

Figure 9. Heat flux (A) and error (B) for temperature distribution *T(x) = 1000+250cos(πx/2)* and concentrations of 5 %, 50 %, 75 % and 100 %.

The average, standard deviation, maximum and minimum values related to the error shown in Fig. 9 are in Tab. 7.

Table 7. Error data associated with the approximation of the heat flux for a homogeneous and non-isothermal medium.

Molar fraction	Average error (%)	Standard deviation of the error	Maximum error (%)	Minimum error (%)
5 %	0.0439	0.0055	0.0568	0.0355
50 %	0.0548	0.0102	0.0793	0.0463
75 %	0.1050	0.0247	0.1586	0.0826
100%	0.1504	0.0379	0.2284	0.1142

The results for the divergence of the heat flux and the error associated with the approximation for a homogeneous and non-isothermal layer with length L = 0.2 m, temperature distribution of *T(x) = 1000+250cos(πx/2)* in Kelvin and wall temperatures of T_0 = 1750 K and T_L = 750 K presented by Solovjov and Webb (2009), are presented in Fig. 10 for molar fractions of 5 %, 50 %, 75 % and 100 %.

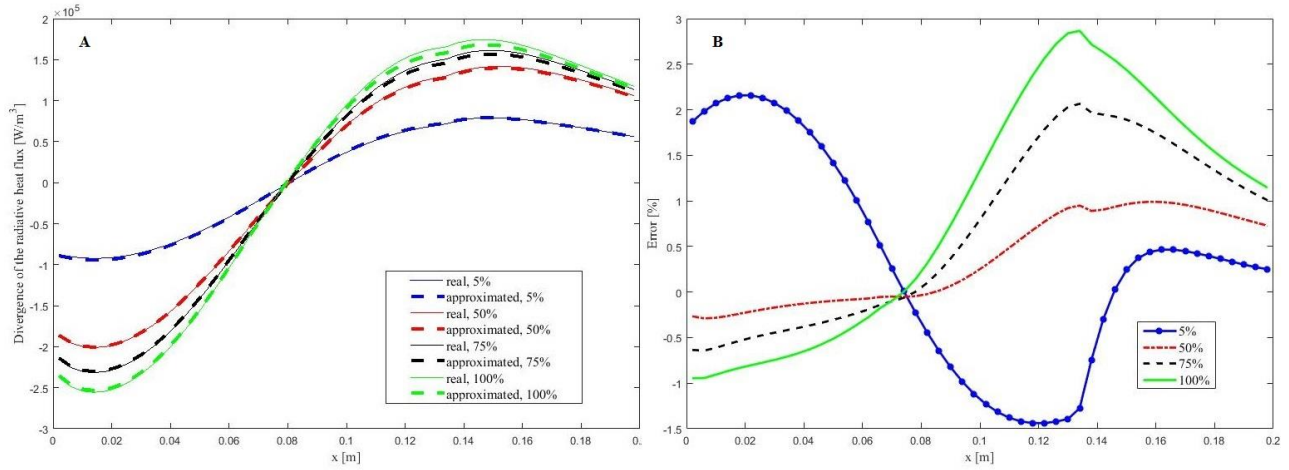

Figure 10. Divergences of the Heat flux (A) and error (B) for temperature distribution *T(x) = 1000+250cos(πx/2)* and concentrations of 5 %, 50 %, 75 % and 100 %.

The average, standard deviation, maximum and minimum values related to the error shown in Fig. 10 are in Tab. 8.

Table 8. Error data associated with the approximation for divergence of the heat flux for a homogeneous and non-isothermal medium.

Molar fraction	Average error (%)	Standard deviation of the error	Maximum error (%)	Minimum error (%)
5 %	1.0278	0.6795	2.1580	0.0122
50 %	0.4749	0.3687	0.9905	0.0144
75 %	0.9613	0.6595	2.0660	0.0031
100%	1.3259	0.8414	2.8659	0.0018

By analyzing the results for the isothermal media, it is possible to note that the approach usually improves with increasing temperature. There are few cases where the error increased with temperature. The only cases that the error increased with temperature were: the average error for the temperature of 2500 K and molar fractions of 5 %, 50 % and 75 %, the average error for the temperature of 1500 K and 2500 K and molar fraction of 5 %, and maximum error for 1500 K and molar fractions of 5 % and 50 %. The maximum error analyzed for all temperatures and concentrations for the heat flux was for the temperature of 500 K and for the CO_2 concentration equal to 100 %, and was 4.8089 %. For this case, however, the average error is equal to 1.8639 % with standard deviation of 1.1346. This maximum error occurs in the wall and for most of the cases. The maximum error verified for the divergence of the heat flux was also for the temperature of 500 K and CO_2 concentration of 100 %, and was 3.1744 %. In the Fig. 6 it is possible to observe that this error occurs close to the wall, while in most of the layer the error is less than 0.5 %. The error presents values smaller than 2 % for the central region of the layers.

The analysis for non-isothermal and uniform media showed that the maximum error for the heat flux was 0.2284 % for the concentration of 100 % while for the divergence of the heat flux it was 2.8659 % for the concentration of 100 %. The average error for the heat flux for all concentrations was less than 1%. For the divergence of the heat flux, the average error was of about 1 %.

Thus, the results obtained with the proposed approximation agree with that obtained considering the real mole fraction.

4. CONCLUSION

The analysis showed that accurate results for radiative heat transfer can be obtained for different CO_2 concentrations approximating the absorption cross-section as that obtained for 25 % of CO_2. It was also possible to observe how the error varies with temperature. In the isothermal layers, the errors were higher close to the walls. It should be noted that there exists a jump in temperature between the wall and the medium. When the temperature varies smoothly, as in the case of the non-isothermal layers, the approach became very accurate, even close to the walls. The approximation was also more accurate in the center of the layer for the non-isothermal case.

Finally, it can be concluded that for the analyzed cases, the proposed approximation was able to provide accurate results.

5. ACKNOWLEDGEMENTS

This work was supported by CNPq, under contract 446281/2014-0, and CAPES/FAPER throughout a scholarship grant for the second author.

6. REFERENCES

Denison MK, Webb BW, 1993b. *An absorption-line blackbody distribution function for efficient calculation of gas radiative transfer*. J Quant Spectrosc Radiat Transfer 50, 499-510.

Denison, M.K., Webb, B.W., 1993a. *A spectral line based weighted-sum-of-gray-gases model for arbitrary RTE solvers*, J. Heat Transfer 115 (4). 1004–1012.

Galarça, M.M., Mossi, A., França, F.H.R., 2011. *A modification of the cumulative wavenumber method to compute the radiative heat flux in non-uniform media*, J. Quant. Spectrosc. Radiat. Transfer 112 (3). 384–393.

Hottel, H.C., Sarofim, A.F., 1967. *Radiative Transfer*, McGraw-Hill, New York.

Howell JR, Meng¨uc¸ MP. Siegel R, 2016. *Thermal Radiation Heat Transfer*. 6th ed. Taylor & Francis Group, New York.

Modest MF, 2013. *Radiative Heat Transfer*. 3th ed. Academic Press, New York.

Modest, M.F., Singh, V., 2005. *Engineering correlations for full spectrum k-distribution of H2O from HITEMP spectroscopic databank*, J. Quant. Spectrosc. Radiat. Transfer 93 (1–3). 263–271.

Modest, M.F., Zhang, H., 2002a. *The full-spectrum correlated-k distribution for thermal radiation from molecular gas–particulates mixtures*, J. Heat Transfer 124 (1). 30–38.

Modest, M.F., Zhang, H., 2002b. *A multi-scale full-spectrum correlated-k distribution for radiative heat transfer in inhomogeneous gas mixtures*, J. Quant. Spectrosc. Radiat. Transfer 73 (2–5). 349–360.

Patankar, S.V., 1980. *Numerical Heart Transfer and Fluid Flow*. Hemisphere.

Pierrot, L., Soufiani, A., Taine, J., 1999. *Accuracy of narrow-band and global models for radiative transfer in H2O, CO2, and H2O–CO2 mixtures at high temperature*, J. Quant. Spectrosc. Radiat. Transfer 62 (5). 523–548.

Rivière, P., Soufiani, A., Perrin, M.Y., Riad, H., Gleizes, A., 1996. *Air mixture radiative property modelling in the temperature range 10,000–40,000 K*, J. Quant. Spectrosc. Radiat. Transfer 56 (1). 29–46.

Rothman LS et al, 2010. *The high-temperature molecular spectroscopic database*. J Quant Spectrosc Radiat Transfer 111, 2139-2150.

Solovjov, V.P., Lemonnie, D., Webb, B.W., 2011. *SLW-1 modeling of radiative heat transfer in nonisothermal nonhomogeneous gas mixtures with soot*, J. Heat Transfer 133 (10). 102701(1–9).

Solovjov, V.P., Webb, B.W., 2002. *A local-spectrum correlated model for radiative transfer in non-uniform gas media*, J. Quant. Spectrosc. Radiat. Transfer 73 (2–5). 361–373.

Solovjov, V.P., Webb, B.W., 2010. *Application of CW local correction approach to SLW modeling of radiativetransferinnon-isothermalgaseousmedia*, Journal of Quantitative Spectroscopy & Radiative Transfer 111. 318–324

7. RESPONSIBILITY NOTICE

The authors are the only responsible for the printed material included in this paper.